Active Damping Method Equivalent to Series Resistor Effect for LCL Filters in a Grid-connected PWM Converters

Byung-Geuk Cho[1], Younggi Lee[2], and Seung-Ki Sul[2]
[1] LS IS Co., Ltd, Anyang, Korea
[2] Seoul National University, Seoul, Korea

***Abstract*-- This paper proposes an active damping method for LCL filters of grid-connected converters. LCL filters are mainly utilized for the interface of distributed generation systems to the grid due to their small size and effectiveness of current harmonics attenuation. However, owing to the resonance of LCL filters, bandwidth of the current controller of the converters is usually limited far to the resonant frequency of the LCL filter. Otherwise, the system stability would be threatened, especially in high power systems where switching frequency and internal loss are relatively low. In this paper, an active damping method equivalent to the implementation of resistors in series to the filter capacitors is suggested and it is shown that the bandwidth of the LCL filter with the proposed damping method can be extended further than that with a conventional capacitor current feedback type damping method. The effectiveness of the proposed method is experimentally confirmed with a 5kW battery energy storage system connected to the grid.**

***Index Terms*— LCL filter, active damping, grid-connected converter, capacitor current feedback.**

I. INTRODUCTION

PWM converters are generally applied to the connection of renewable energy sources such as wind and photovoltaic power systems to the existing grid [1]. For the operation of the grid-connected PWM converters, LCL filters are usually implemented to suppress the current harmonics at the switching frequency and its multiples owing to the small size compared to other filters. However, LCL filters suffer from the resonance effect and it threatens the stability of the system and limits the bandwidth of the current regulator of the converter. Therefore numerous researches have been reported to prevent the resonance phenomenon [2-3].

There are two different damping methods, which are passive and active. Passive damping methods are known to be simple but produce losses and thus the system efficiency would be degraded. On the other hand, active damping methods suppress the resonance by modifying the current controller and can be implemented without any additional loss, which lead to vigorous application for the grid-connected PWM converters though its implementation is tricky.

In this paper, an active damping method equivalent to the implementation of resistors in series to the filter capacitors is proposed. It is proved that the bandwidth of the current regulator of the converter with the proposed active damping method can be extended further than that of a conventional capacitor current feedback type damping method. The effectiveness of the proposed method is explained through Bode plot analysis and confirmed by experimental test with a 5kW battery energy storage system connected to the grid.

II. SYSTEM CONFIGURATION WITH LCL FILTER

The system dealt in this paper is a typical three phase 2 level PWM converter and DC voltage source is supplied by a battery. Its configuration with the grid connection is depicted in Fig. 1.

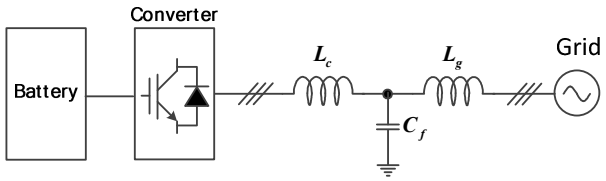

Fig. 1. System configuration of a grid-connected PWM converter

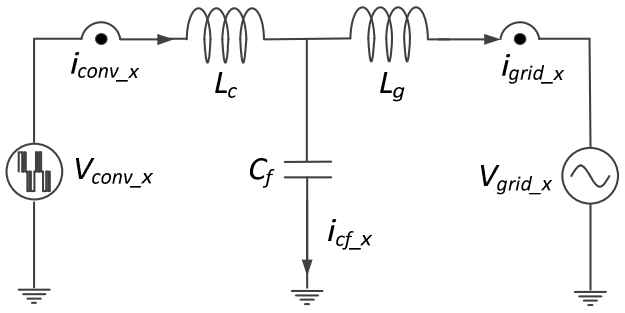

Fig. 2. Single phase equivalent circuit of the system.

The LCL filter is configured with converter side inductor (L_c), grid side inductor (L_g) and the filter capacitor (C_f) as in a single phase equivalent circuit of Fig. 2. V_{conv_x} and V_{grid_x} stand for the converter output voltage and grid voltage, respectively while i_{conv_x}, i_{grid_x}

and i_{cf_x} represent the converter current, grid current and filter capacitor current, respectively. The transfer function of the grid current to the converter output voltage is derived in (1) and the Bode plot of Fig. 3 shows a peak value at the resonant frequency. Then it indicates that the impedance of the filter is theoretically zero at the resonant frequency and hence the grid current diverges even with very small amount of voltage harmonics from the converter at the resonant frequency. Therefore, for the improvement of the stability of the grid current regulator, damping strategies are needed to suppress the resonance phenomenon.

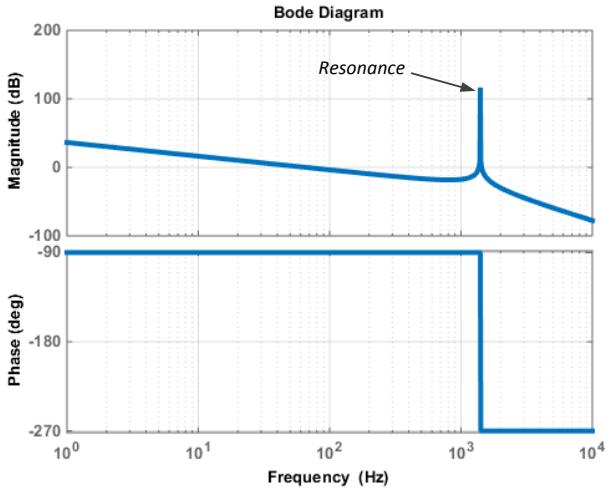

Fig. 3. Bode plot of (1) in LCL filter.

$$\frac{i_{grid\_x}}{V_{conv\_x}} = \frac{1}{s^3 C_f L_c L_g + s\left(L_c + L_g\right)} \tag{1}$$

III. Conventional Passive Damping

As the passive damping methods are the motivation of the proposed active damping method in this paper, the representative conventional passive damping schemes are roughly introduced.

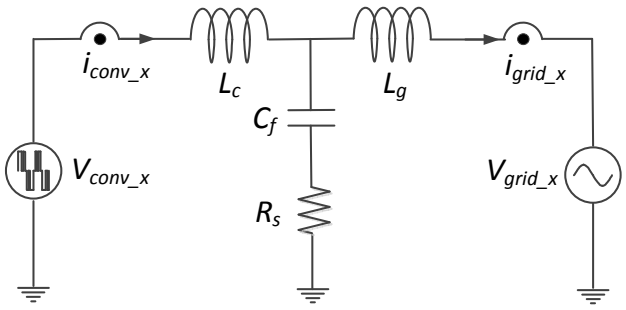

Fig. 4. Passive damping method with a resistor in series to filter capacitor.

Passive damping methods can be divided by the ways of inserting the resistors into the LCL filter. In Fig. 4, the equivalent circuit of the series resistor implementation to the filter capacitor is displayed. Due to the damping resistor, R_s, the transfer function of the grid current to the converter output voltage is adjusted from (1) to (2). As shown in (2), the second order component is added in the denominator and it achieves the damping effect.

$$\frac{i_{grid\_x}}{V_{conv\_x}} = \frac{sC_f R_s + 1}{s^3 C_f L_c L_g + s^2 C_f R_s \left(L_c + L_g\right) + s\left(L_c + L_g\right)} \tag{2}$$

In this passive method, the attenuation slope of the LCL filter is reduced from -60dB/dec to -40dB/dec and thus the switching ripple components are less suppressed as compared to the case of no passive damping filter.

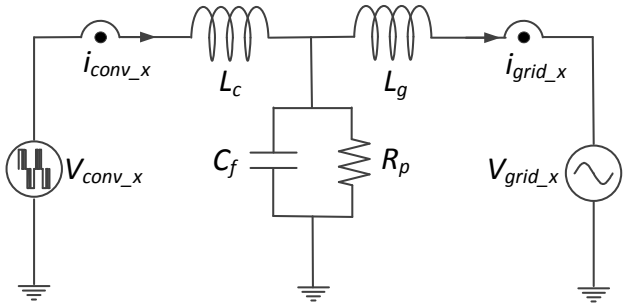

Fig. 5. Passive damping with a resistor in parallel to filter capacitor.

$$\frac{i_{grid\_x}}{V_{conv\_x}} = \frac{1}{s^3 C_f L_c L_g + s^2 \dfrac{L_c L_g}{R_p} + s\left(L_c + L_g\right)} \tag{3}$$

Another major passive damping method is to insert a resistor in parallel to the filter capacitor as in Fig. 5. Then, the transfer function of the grid current to the converter output voltage is altered from (1) to (3). In the range of the resonant frequency, the impedance of the parallel resistor, R_p, is smaller than that of the filter capacitor and consequently resonance is suppressed. In addition, in the range of switching frequency, as the impedance of the filter capacitor is smaller than that of the parallel resistor, the characteristics of the original LCL filter is maintained and hence the attenuation slope is still -60dB/dec, which leads to the proper switching harmonics suppression. However, as the loss from the parallel resistor is mostly larger than the case of the series resistor method, parallel resistor insertion is less often considered for the passive damping schemes [4].

IV. Conventional Active Damping

The active damping methods are to achieve virtual resistor effects by modifying the structure of the regulator. For the implementation of the active damping, the filter capacitor current with a proportional gain (K_d) is

normally used by adding to the converter voltage reference ($_{Vconv\_ref}$) as shown in Fig. 6 [5-7]. When the PWM voltage synthesis is assumed to be unity gain, then the transfer function of the grid current to the converter voltage reference is modified from (1) to (6) by applying (4) and (5). As seen in the denominator of (6), a damping effect is achieved with the added second order component and it is identified by Bode plot of Fig. 7 of the modified transfer function.

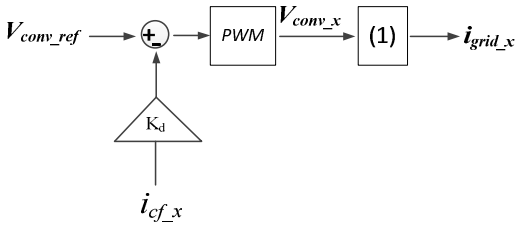

Fig. 6. Conventional active damping with filter capacitor current feedback.

$$\left(V_{conv\_ref} - K_d i_{cf\_x}\right)\frac{1}{s^3 C_f L_c L_g + s\left(L_c + L_g\right)} = i_{grid\_x} \quad (4)$$

$$i_{cf\_x} = s^2 C_f L_g i_{grid\_x} \quad (5)$$

$$\frac{i_{grid\_x}}{V_{conv\_ref}} = \frac{1}{s^3 C_f L_c L_g + s^2 K_d C_f L_g + s\left(L_c + L_g\right)} \quad (6)$$

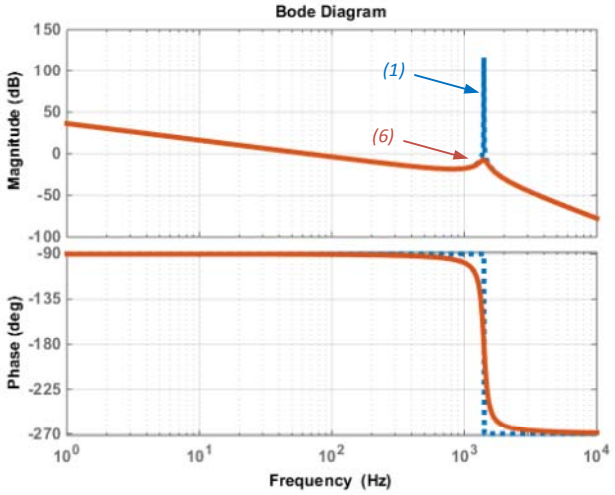

Fig. 7. Effect of a conventional active damping method.

The conventional active damping method can be interpreted by a virtual passive damping scheme. When a resistor is inserted in parallel to the filter capacitor for the passive damping as shown in Fig. 5, the transfer function of the grid current to the converter output voltage is expressed as (3). By comparing (3) and (6) when the PWM gain is unity, it is noticed that the active damping method with the conventional filter capacitor current feedback in Fig. 6 is equivalent to the passive damping method with a resistor in parallel to the filter capacitor as shown in Fig. 5. Therefore, the feedback gain, K_d, for the active damping in the conventional method can be determined as (7) by selecting the appropriate magnitude of the parallel damping resistor, R_p.

$$K_d = \frac{L_c}{C_f R_p} \quad (7)$$

V. Proposed Active Damping

In this paper, an active damping method equivalent to the passive damping with a resistor in series to the filter capacitor is proposed. In the case of the series resistor damping as shown in Fig 4, the transfer function of the grid current to the converter output voltage can be expressed as (2). To realize the equivalent effect in a way of active damping, the implementation of the proposed method can be accomplished by modifying (2) to (8) and the structure of the regulator is depicted in Fig. 8. The gains are determined as in (9) and (10) to achieve the same effect of the series damping resistor, R_s.

$$\frac{V_{conv\_ref} + sC_f R_s V_{conv\_ref} - \dfrac{R_s\left(L_c + L_g\right)}{L_g} i_{cf\_x}}{s^3 C_f L_c L_g + s\left(L_c + L_g\right)} = i_{grid\_x} \quad (8)$$

$$K_{d1} = C_f R_s \quad (9)$$

$$K_{d2} = \frac{R_s\left(L_c + L_g\right)}{L_g} \quad (10)$$

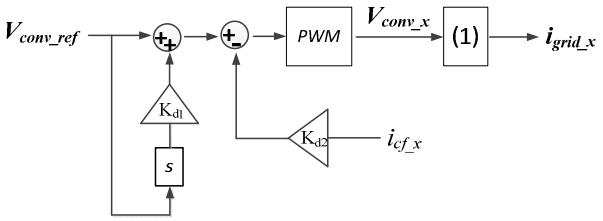

Fig. 8. Implementation of proposed method.

$$\left|\frac{i_{grid}}{V_{conv\_ref}}\right| = \left|\frac{1}{-\omega_{res}{}^2 \dfrac{L_c L_g}{R_p} + j\left(L_c + L_g\right)\omega_{res} - jC_f L_c L_g \omega_{res}{}^3}\right| = 10^{\frac{-GM}{20}} \quad (11)$$

$$\Rightarrow R_p = \frac{\left(L_c + L_g\right)}{C_f} 10^{\frac{-GM}{20}} = 35.67[\Omega]$$

To compare the proposed method and the conventional method, applicable current control bandwidth is investigated. For the same amount of resonant damping, each gain for the proposed method and the conventional method is designed to have 10dB of gain margin (GM) at the resonant frequency. The magnitude of the virtual

resistors in the conventional method and the proposed method are derived as in (11) and (12), respectively.

$$\left|\frac{i_{grid}}{V_{conv\_ref}}\right| = \left|\frac{1+j\omega_{res}C_fR_s}{-\omega_{res}^{\ 2}C_fR_s\left(L_c+L_g\right)+j\left(L_c+L_g\right)\omega_{res}-jC_fL_cL_g\omega_{res}^{\ 3}}\right|$$
$$=10^{\frac{-GM}{20}}$$
$$\Rightarrow R_s = \sqrt{\frac{1}{\omega_{res}^{\ 4}C_f^{\ 2}\left(L_c+L_g\right)^2 10^{-\frac{GM}{10}}-\omega_{res}^{\ 2}C_f^{\ 2}}} = 0.7875[\Omega] \quad (12)$$

The PI controller is normally applied for the regulation of the current in the LCL filter. The gains of the PI controller are designed with an L approximation of the LCL filter [8] because the low frequency behavior of the LCL filter is corresponding to the L filter. Therefore, the reliability and stability of the current regulator including the active damping scheme is dependent on the accuracy of the approximation between the LCL filter and L filter [9].

The model of the L filter for the approximation of the LCL filter is given in (13). Thus, by comparing (2) and (6) to (13), the improvement of the proposed active damping method can be identified.

$$\frac{i_{grid\_x}}{V_{conv\_ref}} = \frac{1}{s\left(L_c+L_g\right)} \quad (13)$$

The Bode plots of the L filter and the LCL filter with the conventional and proposed active damping methods are depicted in Fig. 9. As seen, the models of the LCL filter starts to deviate from that of the L filter at a certain frequency, which may threaten the stability of the PI current controller. Consequently, the bandwidth of the regulator is limited by the deviation for each active damping method.

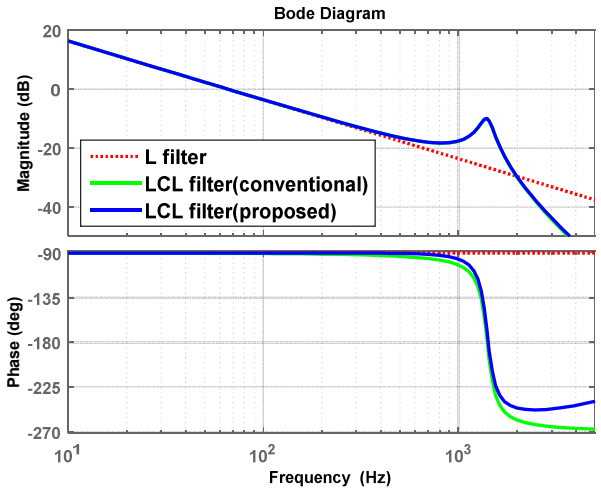

Fig. 9. Comparisons in Bode plot between conventional method and proposed method to L filter.

$$E_{rr\_mag\_conv} = 20\log\frac{|(6)|}{|(13)|} \quad (14)$$

$$E_{rr\_mag\_prop} = 20\log\frac{|(2)|}{|(13)|} \quad (15)$$

$$E_{rr\_ph\_conv} = -90^o - \angle(6) \quad (16)$$

$$E_{rr\_ph\_prop} = -90^o - \angle(2) \quad (17)$$

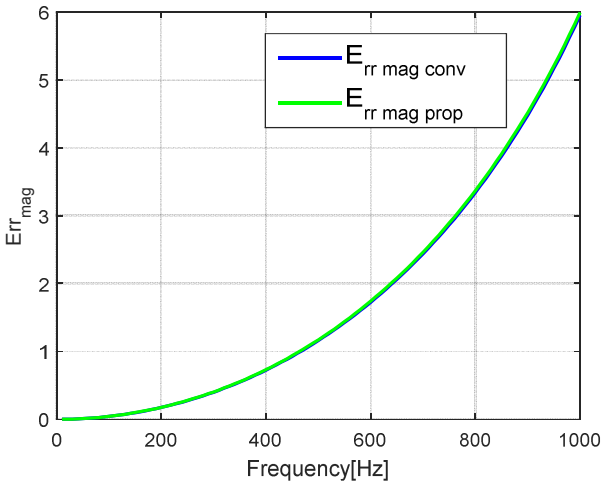

(a)

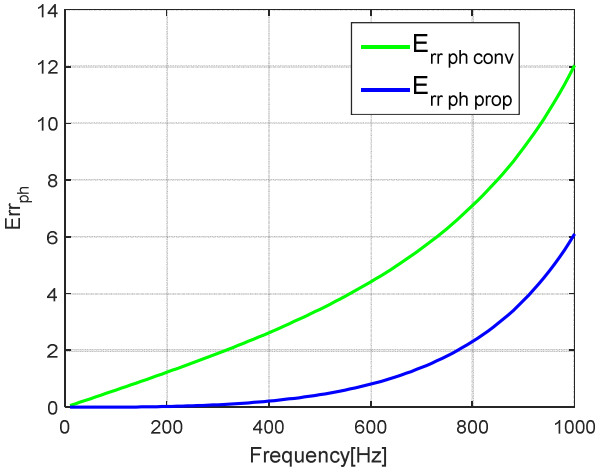

(b)

Fig. 10. Differences between L filter and LCL filter with conventional method and proposed method in terms of (a) magnitude and (b) phase.

For the clear comparison, the differences between the L filter and the LCL filter with the conventional and the proposed active damping methods are investigated in Fig. 10. The deviations in the magnitude and the phase are defined as in (14) ~ (17). In terms of the magnitude as shown in Fig. 10(a), the deviations up to 1kHz are almost the same for the two active damping schemes. However, in the phase deviations point of view as depicted in Fig. 10(b), the proposed method always shows less deviation

compared to the conventional method. This means that the effectiveness of the PI current controller is enhanced and accordingly the bandwidth of the controller can be extended in the proposed active damping method under the same degree of phase error with the conventional active damping method.

In short, it is expected that implementation of an active damping method equivalent to the insertion of a series resistor to the filter capacitor provides superior dynamic performance and stability for the current regulator to the conventional active damping method dealt in IV.

In the meanwhile, the proposed active damping method requires a derivative function. The derivative function threatens the stability and reliability of the system because it amplifies the unnecessary noise components. Therefore the derivative function is replaced by high pass filter for the proposed method as shown in Fig. 11 which is a combination of a derivative function and low pass filter. ω_{der} in (18) stands for the cutoff frequency of the high pass filter.

$$s \approx s\frac{\omega_{der}}{s+\omega_{der}} \tag{18}$$

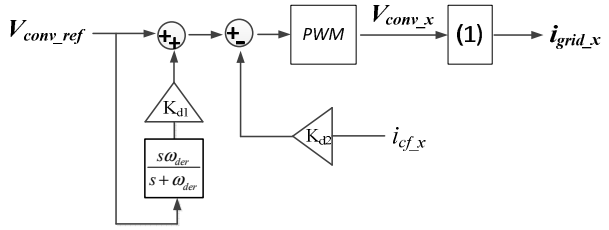

Fig. 11. Implementation of proposed method with high pass filter.

The high pass filter instead of the original derivative function may degrade the performance of the proposed active damping method. The transfer function of the grid current to the converter output voltage is changed from (2) to (19). To notify the effect of the high pass filter, Bode plot of (19) with different cutoff frequency is depicted in Fig. 12. Then it is shown that the phase error to 90° of the L filter increases as the cutoff frequency becomes lower. However, as compared to the conventional method, the phase error is still smaller and thus wider bandwidth for the current regulator can be expected.

$$\begin{aligned}
&\frac{i_{grid_x}}{V_{conv_ref}} = \frac{N(s)}{D(s)}, \\
&N(s) = s\left(\omega_{der}C_f R_s + 1\right), \\
&D(s) = s^4 C_f L_c L_g + s^3 C_f\left[\omega_{der}L_c L_g + R_s\left(L_c + L_g\right)\right] \\
&+s^2\left(L_c + L_g\right)\left(\omega_{der}C_f R_s + 1\right) + s\omega_{der}\left(L_c + L_g\right)
\end{aligned} \tag{19}$$

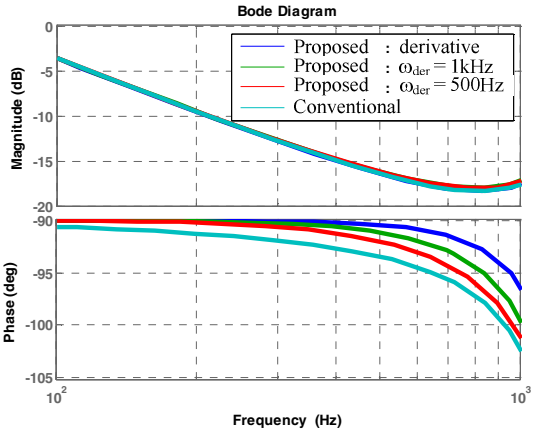

Fig. 12. Effect of high pass filter in the proposed method with different cutoff frequency.

VI. Experimental Results

TABLE I.
System Specification

Rated line to line grid voltage	220[V]
Rated grid current	18.55[A]
Rated DC link voltage	414.4[V]
Switching frequency	5[kHz]
L_c	1.065[mH] / 0.0415[p.u.]
L_g	1.36 [mH] / 0.0532[p.u.]
C_f	21.5[μF] / 0.0785[p.u.]
Resonant frequency	1.48[kHz]

To verify the proposed method, experiments are carried out with 5kW battery energy storage as shown in Fig. 13. The parameters for the experimental setup are shown in TABLE I. To compare the performance of the proposed method to the conventional method, waveforms of the grid currents with different bandwidth of the current regulator are investigated.

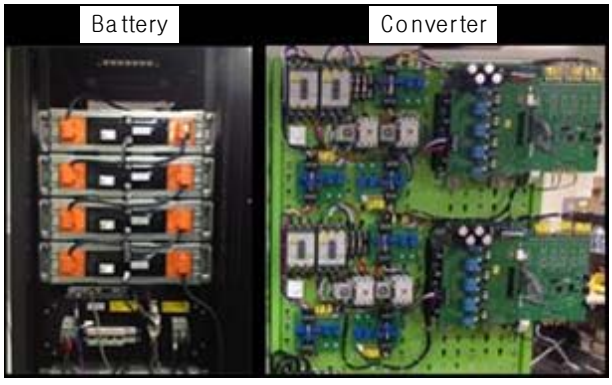

Fig. 13. Experimental setup.

To see the effect of the active damping in the LCL filter, the performance of the current regulator without any active damping method is first identified. It is equivalent to the proportional gain (K_d) to be null in the conventional method in Fig. 6. The waveforms of the grid current are displayed in Fig. 14 with different bandwidths of the current regulator. The results demonstrate that the

grid current is stably regulated with less than 400Hz of the bandwidth but harmonics from the resonance are getting severe as the bandwidths increase over 500Hz.

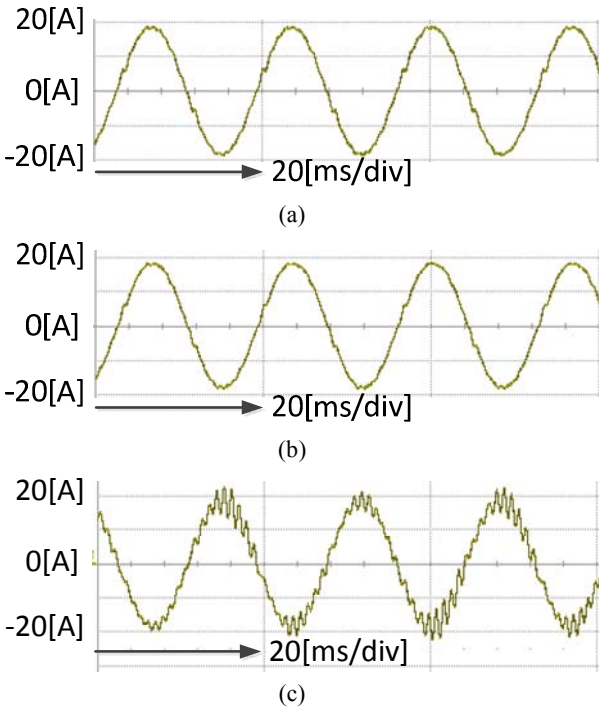

Fig. 14. Waveforms of the grid current without any active damping with bandwidth of (a) 300Hz, (b) 400Hz and (c) 500Hz.

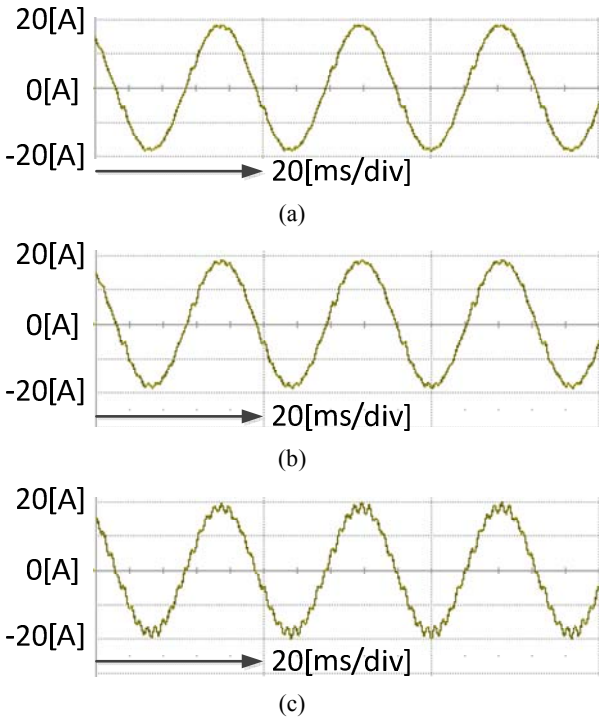

Fig. 15. Waveforms of the grid current for the conventional damping method with bandwidth of (a) 400Hz, (b) 500Hz and (c) 600Hz.

In Fig. 15, the performance of the conventional active damping method is shown. Due to the implemented active damping function, the waveform of the grid current with the bandwidth of 500Hz has less harmonics than the case of no active damping in Fig. 14. However, the damping effect is diminished as the bandwidth is larger than 600Hz.

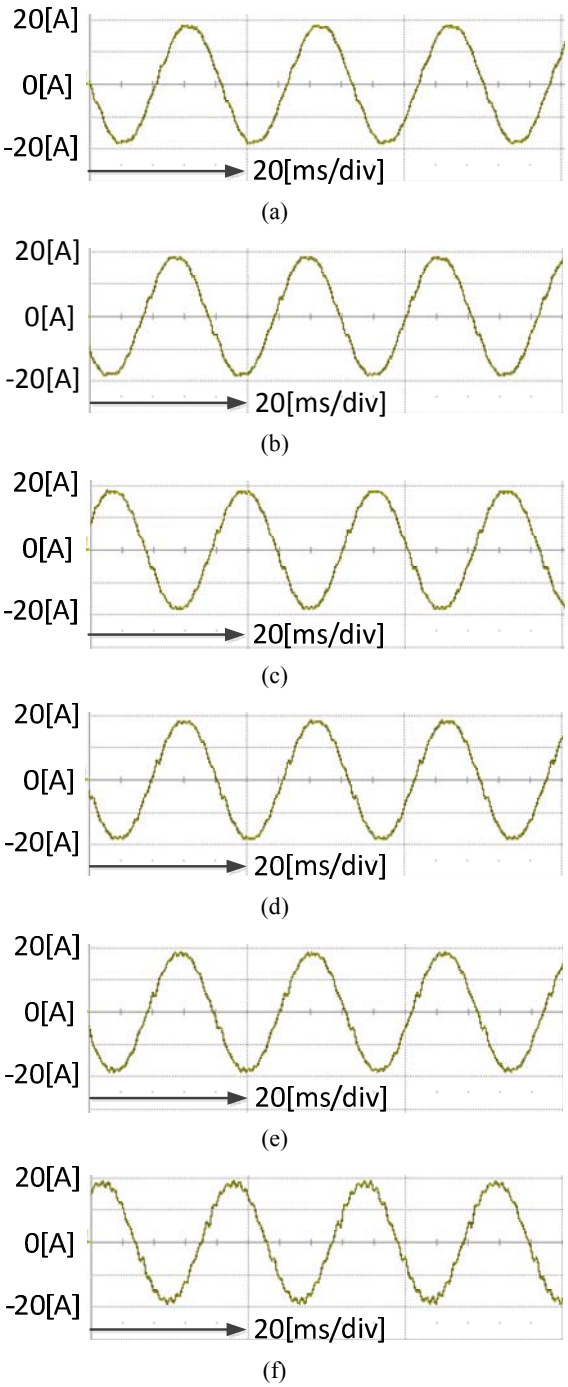

Fig. 16. Waveforms of the grid current for the proposed damping method with bandwidth of (a) 500Hz, (b) 600Hz ,(c) 700Hz, (d) 800Hz, (e) 900Hz and (f)1kHz.

In Fig. 16, the performance of the proposed active damping method is shown. The bandwidth of the current regulator is increased from 500Hz to 1kHz. In the proposed method, the grid current includes less resonant

harmonics at the same bandwidth compared to the conventional method. Therefore, it can be said that bandwidth of the current regulator with the proposed active damping method is extended compared to that of the conventional method. The bandwidth has been extended by 80% from 500Hz to 900Hz and it can be shown in Fig. 17 for the same phase deviations for the conventional method and the proposed method from the L filter model.

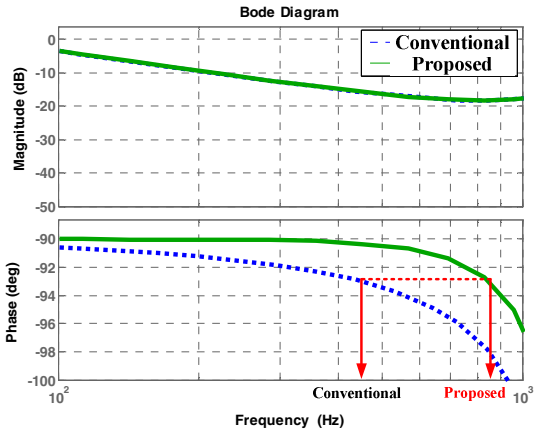

Fig. 17. Increased bandwidth effect in proposed method.

To see the dynamic performance of the current regulator with the proposed method, the step responses are investigated. The results for the step up responses and the step down responses in the synchronously rotating d-q reference frame are displayed in Fig. 18 and Fig. 19. i_{dsr_ref} and i_{qsr_ref} stand for the grid currents references whereas i_{dsr} and i_{qsr} represent the actual grid currents in the synchronous reference frame. To compare the performance of the proposed method to the cases of no active damping and the conventional method against the resonance, the bandwidth of the current regulator in each case is set the same and the transient states are analyzed. Due to the same bandwidth of the current regulator, the settling times in the three cases are almost equal. However, the regulation error of the case with the proposed damping method is the least. From the experimental results, it can be said that the proposed method achieves the best regulation performance in the suppression of the resonant harmonics.

VII. Conclusions

In this paper, an active damping method equivalent to the insertion of series resistor to the capacitor of LCL filter has been proposed. Through the analysis of the model error for the current controller, the proposed method provides wider range of bandwidth than the conventional method. It has been experimentally confirmed that the bandwidth of the current regulator of the converter with the proposed damping method can be extended by 80% compared to that of a conventional capacitor current feedback type active damping method. In addition, the resonant damping effect is also identified in the transient state and the effectiveness of the proposed method is validated.

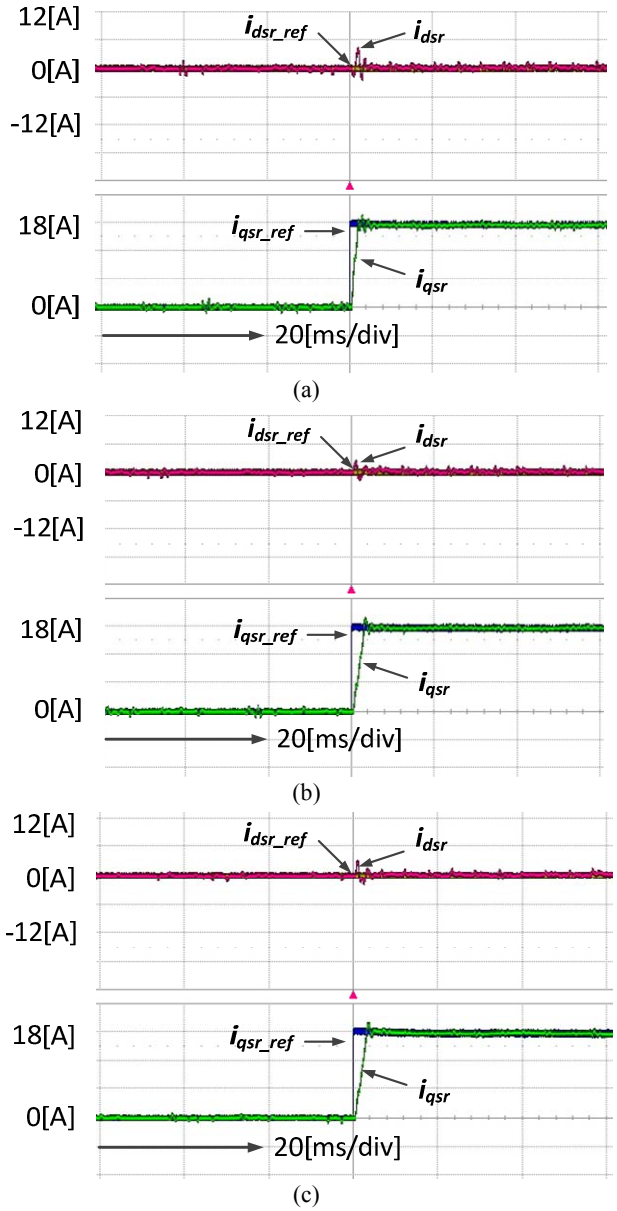

Fig. 18. Step up responses of (a) no active damping case, (b) conventional active damping method and (c) proposed active damping method.

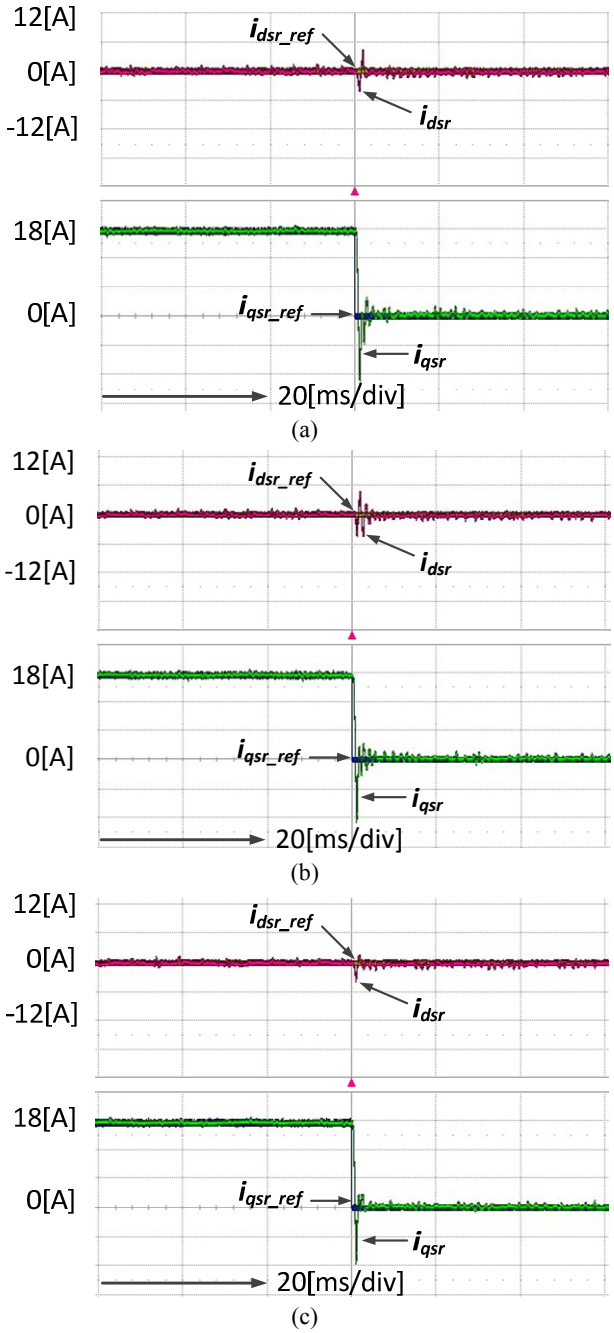

Fig. 19. Step down responses of (a) no active damping case, (b) conventional active damping method and (c) proposed active damping method

REFERENCES

[1] G.M. Masters, Renewable and efficient electric power systems : John Wiley & Sons, 2013.

[2] H. Jinwei and L. Yun Wei, "Generalized Closed-Loop Control Schemes with Embedded Virtual Impedances for Voltage Source Converters with LC or LCL Filters," *Power Electronics, IEEE Transactions on,* vol. 27, pp. 1850-1861, 2012.

[3] Malinowski M., Bernet S., "A Simple Voltage Sensorless Active Damping Scheme for Three-Phase PWM Converters With an LCL Filter," *Industrial Electronics, IEEE Transactions on* , vol.55, no.4, pp.1876,1880, April 2008.

[4] C. Byung-Geuk and S. Seung-Ki, "LCL filter design for grid-connected voltage-source converters in high power systems," in *Energy Conversion Congress and Exposition (ECCE), 2012 IEEE*, 2012, pp. 1548-1555.

[5] P. Donghua, R. Xinbo, B. Chenlei, L. Weiwei, and W. Xuehua, "Capacitor-Current-Feedback Active Damping With Reduced Computation Delay for Improving Robustness of LCL-Type Grid-Connected Inverter," *Power Electronics, IEEE Transactions on,* vol. 29, pp. 3414-3427, 2014.

[6] S. G. Parker, B. P. McGrath, and D. G. Holmes, "Regions of Active Damping Control for LCL Filters," *Industry Applications, IEEE Transactions on,* vol. 50, pp. 424-432, 2014.

[7] B. Chenlei, R. Xinbo, W. Xuehua, L. Weiwei, P. Donghua, and W. Kailei, "Step-by-Step Controller Design for LCL-Type Grid-Connected Inverter with Capacitor Current-Feedback Active-Damping," *Power Electronics, IEEE Transactions on,* vol. 29, pp. 1239-1253, 2014.

[8] Liserre M., Blaabjerg F., Hansen S., "Design and control of an LCL-filter-based three-phase active rectifier," *Industry Applications, IEEE Transactions on*, vol.41, no.5, pp.1281,1291, Sept.-Oct. 2005.

[9] Dannehl, J.; Wessels, C.; Fuchs, F.W., "Limitations of Voltage-Oriented PI Current Control of Grid-Connected PWM Rectifiers With LCL Filters," *Industrial Electronics, IEEE Transactions on* , vol.56, no.2, pp.380,388, Feb. 2009.